MONITORING RESERVOIR WATER LEVEL AND SURFACE AREA DYNAMICS USING SATELLITE ALTIMETRY AND OPTICAL IMAGERY: TSALKA RESERVOIR, GEORGIA

Nika TKESHELASHVILI [1*], ***Tamar PAPACHASHVILI*** [1] ***& Giorgi BREGVADZE*** [2]

DOI: 10.21163/GT_ GT_2026.213.06

ABSTRACT

Monitoring of inland water body dynamics is essential for understanding hydrological variability and supporting sustainable management of freshwater resources, especially in regions with limited hydrometric observations. This study evaluates the potential of integrated use of Sentinel-3 radar altimeter data and PlanetScope optical imagery for monitoring surface water area and level parameters of the Tsalka (Khrami) Reservoir in Georgia over the period 2017–2024. Water level time series were derived from Sentinel-3 SRAL data, while reservoir surface area was extracted from PlanetScope imagery. Validation against in situ measurements demonstrates high accuracy of radar altimeter (Bias = 0.097 m, RMSE = 0.192 m, r = 0.997, NSE = 0.993). The results reveal pronounced seasonal and interannual variability of Tsalka Reservoir, with water levels ranging from 1498.86 m to 1508.42 m and surface area from 5.69 km² to 24.54 km². The study confirms that the combined use of altimetry and high-resolution optical data provides a reliable and cost-effective framework for hydrometric monitoring of medium size inland water bodies.

Keywords: *Hydrometric monitoring; Radar altimetry; Optical remote sensing; Tsalka Reservoir.*

1. INTRODUCTION

Effective monitoring of water levels, volumes, and surface area dynamics of freshwater lakes and reservoirs is a fundamental component of sustainable water resources management. It is essential for hydropower plant (HPP) operation, the proper functioning of drinking water and irrigation systems, and for assessing natural and societal risks associated with hydrological processes under ongoing climate change (Wang et al., 2025; Woolway et al., 2020). These issues are aligned with the United Nations Sustainable Development Goals 6, 13, and partially with Goal 14.

Monitoring of inland water resources has traditionally relied on in situ hydrological stations. Data collected from these stations are used to characterize the magnitude of variability and the spatio-temporal dynamics of both quantitative and qualitative parameters of specific water bodies. However, this approach is associated with several limitations, including the sparse distribution of hydrological stations due to high operational costs and the lack of a unified monitoring network. In addition, access to such data is often restricted, and heterogeneity in data types may introduce interoperability challenges (Luo et al., 2022; Chen et al., 2022).

---

[1] *Georgian Technical University, Department of Engineering Geodesy & Geoinformatics, Tbilisi, Georgia.*
[*] *Corresponding author tkeshelashvili.nika@gtu.ge, t.papachashvili@gtu.ge*
[2] *Ivane Javakhishvili Tbilisi State University, Department of Geography, Tbilisi, Georgia, giorgi.bregvadze@tsu.ge*

Georgia is relatively rich in water resources, with more than 26,000 rivers and over 1,350 lakes and reservoirs, including small glacial lakes. Nevertheless, the absence of a unified national water monitoring network remains a significant challenge. In recent years, monitoring conditions have improved for river systems; however, no hydrometric parameters are systematically observed by state institutions for lakes and reservoirs.

In cases where reservoirs are operated by hydroelectric power companies, water level monitoring is conducted by private operators, but such data are generally not accessible to the scientific community, relevant governmental agencies, or the public. For a large proportion of lakes and reservoirs, hydrometric data are entirely lacking, which substantially limits the assessment of freshwater resources, the advancement of scientific research, and effective water resources management. This limitation, in turn, constrains the development of multiple economic sectors dependent on these resources. Consequently, long-term changes in key quantitative indicators of water resources since the collapse of the Soviet Union and the subsequent independence of Georgia remain largely unknown, particularly in the context of ongoing, accelerated environmental and climate changes driven by both anthropogenic and natural factors.

To address these challenges facing the country, it is necessary to develop alternative approaches for water resource monitoring based on modern technologies. In recent years, advances in satellite remote sensing, in particular radar-based systems, have created new opportunities for monitoring the dynamics of inland water bodies with high temporal resolution and extensive spatial coverage. (Kossieris et al., 2024; An et al., 2022). Originally developed for oceanography, radar altimetry is now widely applied to lakes, rivers, and reservoirs, offering continuous observations largely independent of weather conditions and cloud cover (Jamali et al., 2025). Modern missions operating in synthetic aperture radar (SAR) mode, such as Sentinel-3, provide improved spatial resolution and accuracy compared to earlier low-resolution altimeters (Tang et al., 2023; Bazzi et al., 2025). At the same time, optical remote sensing techniques have demonstrated considerable potential for reconstructing long-term lake surface variability and analyzing changes in water extent, even in cases where image availability is limited (Haidu et al., 2024; El Orfi et al., 2025).

A number of recent studies have demonstrated the effectiveness of integrating satellite altimetry and optical remote sensing for inland water monitoring in different environmental settings (Zeng et al., 2023). Nevertheless, despite the increasing use of Sentinel-3 altimetry and PlanetScope imagery independently, studies combining these datasets for integrated assessment of reservoir water level and surface area dynamics remain relatively limited, particularly for small and medium reservoirs located in mountainous regions with complex shoreline morphology and sparse hydrological observations. In contrast, the present study is specifically oriented toward a medium-sized mountainous reservoir located in a region characterized by the absence of a unified inland water monitoring network and limited accessibility of in situ hydrometric data. The scientific contribution of this work therefore lies not only in the application of multi-sensor remote sensing techniques, but also in the adaptation and evaluation of an integrated methodological framework under conditions of strong seasonal shoreline variability, complex surrounding topography, and restricted ground-based observations. In addition, the study represents first long-term satellite-based assessments of reservoir water level and surface area dynamics in Georgia.

Therefore, the aim of this study is to evaluate the potential of integrated use of data from the European Space Agency's Sentinel-3 mission, with high spatial resolution PlanetScope optical imagery provided by Planet Labs, for the seasonal and multi-year monitoring of surface area and level fluctuations of the largest artificial reservoir in Georgia, the Tsalka (Khrami) Reservoir. Tsalka Reservoir, located in the Tsalka Municipality, southern Georgia, represents one of the most significant freshwater resources in the country. Its water is utilized for hydropower generation by three hydroelectric power plants, as well as for agricultural irrigation and fisheries. The primary inflow to the reservoir is provided by the Ktsia–Khrami river system, a transboundary river shared between Georgia and Azerbaijan. In addition, the study seeks to evaluate applicability of proposed methods for the monitoring of other lakes and reservoirs in Georgia within the coverage of these and similar remote sensing missions.

2. STUDY AREA AND DATASETS

2.1. Study area

The Tsalka (Khrami) Reservoir (**Fig. 1**) is located in southern Georgia, within the Kvemo Kartli region, in the central part of the Tsalka volcanic plateau, approximately 100 km southwest of the capital, Tbilisi. The reservoir was constructed in 1946 on the Ktsia–Khrami river system and, with a design surface area of approximately 33 km^2, represents the largest artificial water body in Georgia.

The Tsalka Reservoir is a channel-type reservoir. The steepness of its coastal slopes' ranges from 5° to 90°, reflecting highly variable shoreline morphology. The reservoir has a length of approximately 14.5 km, an average width of 2.4 km, and a maximum width of 3.5 km. Its average depth is 9.3 m, with a maximum depth reaching 25.0 m (Iordanishvili et al., 2023). The reservoir constitutes the central component of the Khrami Hydropower Cascade, supplying water to three hydroelectric power plants. In addition, it is used for irrigation and fisheries, highlighting its importance as a multifunctional freshwater resource at the national scale.

The hydrological regime of the reservoir is primarily controlled by inflows from the Khrami River and its tributaries, supplemented by atmospheric precipitation, snowmelt, and groundwater contributions. The reservoir exhibits pronounced seasonal variability, with water levels typically increasing during spring and early summer in response to snowmelt and elevated river discharge. In contrast, declining water levels are observed during autumn and winter, partly due to regulated outflows associated with hydropower generation.

The climatic conditions of the reservoir area are characterized by cold winters and mild summers. According to ERA5-Land data, the average annual air temperature at 2 m above the surface during the study period (2017–2024) ranges from 6.2 °C to 7.18 °C. Based on GPM data, the average annual precipitation varies between 591.32 mm and 842.14 mm.

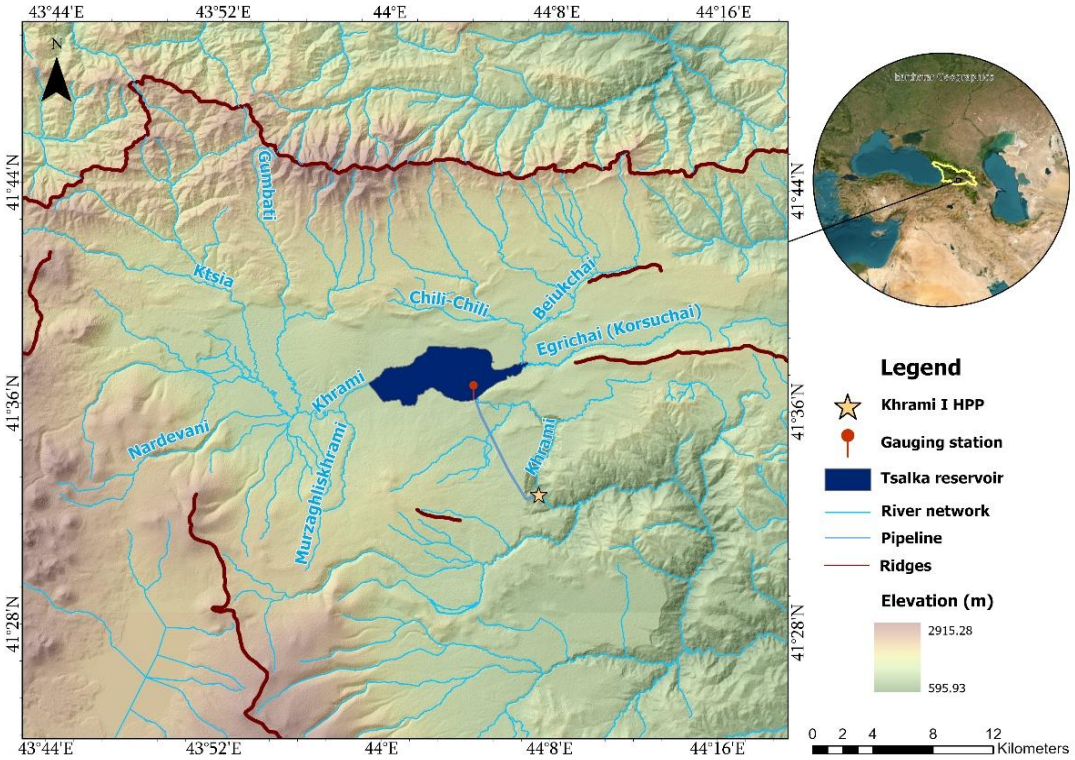

Fig. 1. Study area.

It should be noted that for the characterization of climatic parameters of the study area ERA5-Land and GPM datasets were used because no in situ meteorological observations was available. Although climatic characteristics of the region are discussed in Soviet-era literature, more recent datasets were preferred due to ongoing climate change and the necessity of representing contemporary climatic conditions during the study period. Both ERA5-Land and GPM products are widely used in recent climatological and hydrological studies because of their continuous temporal coverage and suitability for regions with complex topography and sparse observation networks (Dalla Torre et al., 2024; Jawad et al., 2024). The area surrounding the Tsalka Reservoir is sparsely populated. The landscape is predominantly composed of agricultural land and pastures, with steppe-type landscapes prevailing throughout the region. As noted above, under conditions of ongoing climate change and a sparse hydrological monitoring network, the use of satellite altimetry can significantly fill the data gaps. The hydrometric characteristics of the Tsalka Reservoir provide favorable conditions for testing this approach and for its potential integration into a national inland water monitoring system in Georgia.

2.2. Datasets

2.2.1. Sentinel-3 altimetry data

Sentinel-3 is a polar-orbiting, sun-synchronous Earth observation mission (98.6° inclination) developed as part of the European Space Agency's Copernicus Programme, designed to monitor ocean and land topography, land ice, inland waters, and key climate parameters. The first satellite, Sentinel-3A, was launched on 16 February 2016, followed by Sentinel-3B on 25 April 2018, while Sentinel-3C is scheduled for launch in 2026 (https://www.esa.int). The satellites operate at an orbital altitude of approximately 814.5 km, with a 27-day repeat cycle corresponding to 385 orbits per cycle. The Sentinel-3 platform carries three primary instruments: the Synthetic Aperture Radar Altimeter (SRAL), the Ocean and Land Colour Instrument (OLCI), and the Sea and Land Surface Temperature Radiometer (SLSTR). For the purposes of this study, data acquired from the SRAL instrument were used to derive reservoir surface heights. SRAL is a radar altimeter designed to measure surface elevations over oceans, ice sheets, rivers, and lakes. It operates as a dual-frequency sensor, utilizing Ku and C bands. The Ku band (≈13.57 GHz) provides the primary ranging measurements, while the C band (≈5.41 GHz) is used to correct for ionospheric delays. After SAR processing, the along-track spatial resolution of the sensor is approximately 300 m.

Sentinel-3 data used in this study were obtained from the French Centre for Ocean and Hydrosphere Topography (CTOH - https://www.legos.omp.eu/ctoh/) (requested and accessed on 21 May 2025). For the Tsalka Reservoir, measurements from track 526 were used for the period January 2017 to December 2024. However, at the time of the data acquisition, measurements for three months in 2024 (May–July) were not available; therefore, the analysis was performed excluding these data.

2.2.2. PlanetScope Imagery

The optical imagery used in this study was obtained under the Education and Research Program license of Planet Labs PBC. During the study period, the PS-2 four-band surface reflectance product was used for extraction of the monthly water-covered area of the Tsalka Reservoir. The imagery has a spatial resolution of 3 m and a radiometric resolution of 12 bits. The Dove/PS-2 satellites are equipped with four spectral bands covering the blue (455–515 nm), green (500–590 nm), red (590–670 nm), and near-infrared (780–860 nm) regions of the electromagnetic spectrum. This product is geometrically and atmospherically corrected.

PlanetScope's revisit time of approximately 1 day is particularly advantageous for this type of analysis. Its high temporal resolution enables the acquisition of multispectral imagery of the reservoir closely matching the Sentinel-3 altimetry measurement dates, thereby allowing accurate extraction of the water-covered area. In recent years, PlanetScope imagery has also been successfully applied in

Georgia and the Greater Caucasus region for glacier and proglacial lake mapping, highlighting its suitability for monitoring cryospheric and inland water environments (Tielidze et al., 2025a; Tielidze et al., 2025b).

2.2.3. In situ measurements

As noted, hydrometric parameters are not systematically monitored by relevant state institutions for lakes and reservoirs in Georgia. The Tsalka Reservoir forms part of the infrastructure of the Khrami Hydropower Cascade. In situ daily water level data for the period 2017–2024 were provided by JSC "KHRAMHESI I", the operating company of the Khrami I Hydropower Plant. The data were obtained from a single hydrological station equipped with an automatic level gauge and referenced to mean sea level.

3. METHODS

3.1. Satellite altimetry processing and water level time series extraction

Satellite radar altimeters measure surface elevation by determining the two-way travel time of a microwave pulse between the satellite and the reflecting surface. During propagation through the atmosphere, the radar signal is affected by several atmospheric and geophysical factors, requiring the application of corresponding corrections to obtain accurate surface elevations. Taking these effects into account, the orthometric height (h) of the water surface can be expressed as (Eq. (1)):

$$h = H - R_0 - \Delta R_{corr} - N \tag{1}$$

where, H is the satellite altitude above the reference ellipsoid, R_0 - the measured range at nadir (i.e., the distance between the satellite center and the reflecting surface), ΔR_{corr} represents the sum of applied corrections, and N denotes the geoid undulation. The corrections applied to the H and R have been the focus of several studies in the literature (Frappart et al., 2017).

The total correction term ΔR_{corr} accounts for atmospheric propagation delays and other geophysical effects (Crétaux et al., 2017) (Eq. (2)):

$$\Delta R_{corr} = \Delta R_{iono} + \Delta R_{dry} + \Delta R_{wet} + \Delta R_{solid} + \Delta R_{pole} \tag{2}$$

These components correspond, respectively, to ionospheric delay, dry tropospheric delay, wet tropospheric delay, and solid Earth and pole tide corrections. The application of these corrections is essential, as atmospheric refraction alters the propagation speed of the radar signal, leading to biases in surface height estimation. Tropospheric and ionospheric effects are particularly significant over inland water bodies; therefore, their accurate modeling is important. (Fernandes et al., 2014).

All parameters required for surface elevation retrieval are provided in the Level-2 GDR product provided by CTOH, including the geophysical corrections described above. It should be noted that the Level-2 GDR dataset includes multiple retracking algorithms (ICE-1, Ocean, and Seaice). In this study, the ICE-1 retracker was used, which is based on the Offset Center of Gravity (OCOG) technique. The altimetry data are provided in NetCDF (.nc) format and were processed and analyzed using the Panoply and ALTiS software tools. As previously mentioned, only a single Sentinel-3 ground track (Track 526) intersects the Tsalka Reservoir (**Fig. 2**).

For the construction of the reservoir water level time series, the initial step involved defining a virtual station at the intersection of the satellite ground track and the water surface. The maximum extent of the reservoir during the study period was delineated from a corresponding PlanetScope image and digitized in ArcGIS Pro.

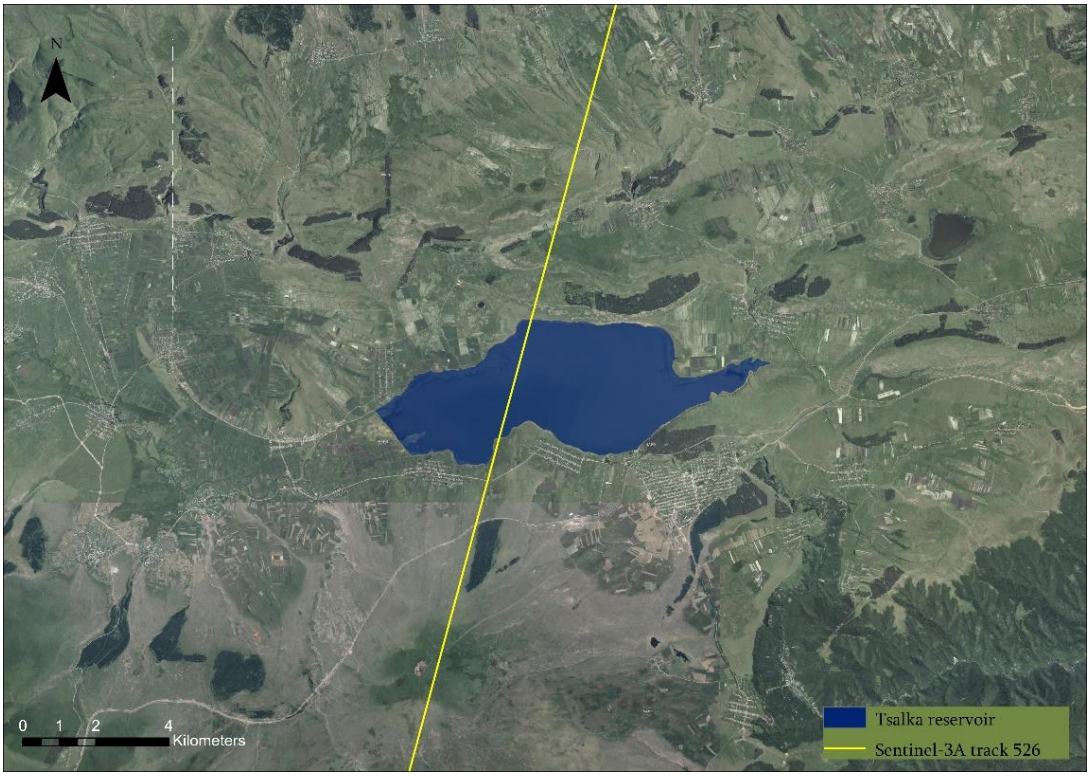

Fig. 2. Sentinel-3A track 526 over Tsalka Reservoir (superimposed on 2016-2017 orthomosaic provided by the National Agency of Public Registry of Georgia)

The resulting polygon was used to define the virtual station, which was subsequently imported into the ALTiS software to extract water level time series. Due to pronounced seasonal variations in the water-covered area of the Tsalka Reservoir, the extracted time series were manually adjusted on a date-specific basis, and altimeter footprints falling outside the water extent were removed. Following this filtering procedure, several altimeter footprints (up to a maximum of 12) remained within the virtual station for each measurement date.

Assuming hydrostatic equilibrium, the free surface of the reservoir represents an equipotential surface and is therefore approximately horizontal under normal conditions, particularly over such a limited spatial extent. Consequently, individual elevation measurements obtained for a given date are expected to be consistent. In practice, however, outliers may occur due to waveform contamination, mixed land–water echoes near the shoreline, surface roughness variations, and retracking inaccuracies. To ensure the reliability of the water level estimates, an outlier detection and removal procedure was applied to each measurement set.

First, the median value ($\tilde{h}$) of the measurements within the virtual station was calculated for each satellite pass. The individual measurements (h), were then compared with the median, and the residuals (r) were computed as the difference between them (Eq. (3)):

$$r = h - \tilde{h} \tag{3}$$

In applying this method, it is necessary to define a tolerance threshold (T) for the residuals. Measurements for which the absolute residual ($|r|$) exceeds T, are classified as outliers and excluded from further analysis. In this study, T was tested within the range of 0.3–0.7 m, and a value of 0.5 m

was selected as optimal. The filtering procedure was applied iteratively, resulting in a consistent cluster of measurements with reduced influence of extreme deviations. After outlier removal, the reservoir water level time series was derived by computing the median of the remaining valid measurements.

The surface elevations derived from the Sentinel-3 radar altimeter are referenced to the WGS84 ellipsoid. To obtain water levels relative to mean sea level, a geoid correction was applied. Geoid undulation values (N) were obtained from the EGM2008-5 global geoid model and subtracted from the ellipsoidal heights. As a result, a time series of orthometric water surface elevations was derived. This transformation is essential for the direct comparison of altimetry-derived results with in situ measurements and for subsequent hydrological analyses.

3.2. Water-covered area extraction

The seasonal and interannual variability of the Tsalka Reservoir surface area was analyzed using PlanetScope surface reflectance imagery for 93 months of the study period. The selection of PlanetScope data is justified by its high spatial resolution (3 m), which enables detailed delineation of the fragmented shoreline. In addition, the high revisit frequency of PlanetScope satellites allows the acquisition of scenes closely matching the Sentinel-3 altimetry measurement dates. For each Sentinel-3 observation month, images were selected within a ±5-day time window to map the water-covered area and minimize temporal discrepancies between water level and surface area estimates.

The Normalized Difference Water Index (NDWI), originally proposed by McFeeters (1996), was used to delineate the water surface of the reservoir. This index is defined as the normalized difference between the green and near-infrared (NIR) spectral bands of multispectral imagery, enhancing the detection of open water bodies. For each PlanetScope image, NDWI was calculated as Eq. (4):

$$NDWI = \frac{Green - NIR}{Green + NIR} \tag{4}$$

For PlanetScope imagery, green corresponds to band 2 and NIR corresponds to band 4. After NDWI computation, a threshold-based classification was applied to separate water from non-water pixels. In general, pixels with positive NDWI values are associated with open water, while negative or low NDWI values correspond to surrounding non-water surfaces. Because spectral conditions varied slightly among acquisition dates, the classification threshold was adjusted individually for each PlanetScope scene. Pixels with NDWI values above the selected thresholds were classified as water, and all remaining pixels were classified as non-water. Derived rasters were vectorized into polygon features. This approach is consistent with previous studies that have applied spectral indices to delineate surface water from optical imagery, including PlanetScope data, and remains an effective method, particularly in the context of high-frequency observations and efficient data processing (Alcaras et al., 2022; Van et al., 2025).

However, this approach is valid under ice-free conditions. During periods when the reservoir is partially covered by ice or snow, automatic spectral separation of water and non-water surfaces becomes less reliable, as frozen water surfaces and snow cover in adjacent areas alter the spectral characteristics of the reservoir. In such cases, the automatically derived water masks were visually inspected and manually refined to obtain shoreline boundaries that more accurately represent the true water extent observed in the imagery (Cheng et al., 2023; Wang et al., 2020). Manual delineation procedures have also been applied in recent studies conducted in the Georgian Caucasus using PlanetScope imagery for mapping proglacial lakes and monitoring glacier changes (Tielidze et al., 2025a). The automated computation of NDWI for the PlanetScope time series was performed in a Python programming environment using Jupyter Notebook. As a result of the above procedures, monthly surface area values were derived for the Tsalka Reservoir, with acquisition dates closely matching the Sentinel-3 measurements.

3.3. Construction of the stage-area curve

The relationship between water level and water-covered area in the Tsalka Reservoir was established using paired observations of water level and surface area derived for the study period, as described in the preceding subsections.

To obtain a continuous functional representation of the relationship between water level and water-covered area, a nonlinear regression model was fitted to the observed data. A four-parameter logistic (4PL) function was employed, as it effectively captures the sigmoidal response characteristic of reservoirs, where the surface area increases slowly at low water levels, more rapidly at intermediate levels, and gradually approaches quasi-asymptotic behavior at higher levels. The model is expressed as Eq. (5):

$$A(L) = A_{min} + \frac{A_{max} - A_{min}}{1 + \exp\left[-k(L - L_0)\right]} \tag{5}$$

where, $A(L)$ represents the reservoir surface area at water level L, A_{min} and A_{max} denote the lower and upper asymptotic limits of the surface area estimated by the model, respectively, k is the growth rate (steepness) of the curve, and L_0 is the inflection point corresponding to the water level at which the rate of area increase is maximal.

Model parameters were estimated using nonlinear least-squares optimization (Eq. (6)), minimizing the sum of squared residuals:

$$S = \sum_{i-1}^{N} [A_i - A(L_i)]^2 \tag{6}$$

where, L_i represents the water level and A_i is the corresponding surface area for observation i.

The fitted function provides a smooth approximation of the discrete observations and enables the estimation of water-covered area for any water level within the observed range. It should be noted that the dataset does not encompass the full range of possible reservoir storage conditions. Accordingly, the asymptotic parameters A_{min} and A_{max} should not be interpreted as the absolute minimum and maximum extents of inundation, but rather as model parameters describing the empirical relationship within the range of water level values considered in this study.

3.4. Quantitative validation of altimetry data accuracy

To quantitatively assess the accuracy of the water level time series derived from the Sentinel-3 radar altimeter, the results were validated against daily in situ observations provided by JSC "KHRAMHESI I" for the corresponding measurement dates.

The systematic deviation between the two datasets was quantified using the mean bias error (Bias), defined as Eq. (7):

$$Bias = \frac{1}{n} \sum_{i=1}^{n} (A_i - G_i) \tag{7}$$

where, A_i represents the water level derived from the radar altimeter and G_i denotes the corresponding in situ measurement. Ideally, the resulting value should be close to zero.

To quantify the magnitude of the absolute discrepancy, the root mean square error (RMSE) was used, calculated as follows (Eq. (8)):

$$RMSE = \sqrt{\frac{1}{n} \sum_{i=1}^{n} (A_i - G_i)^2} \tag{8}$$

The strength of the linear relationship between altimetry-derived and in situ water levels was quantified using the Pearson correlation coefficient (Eq. (9)):

$$r = \frac{\sum_{i=1}^{n}(A_i-\bar{A})(G_i-\bar{G})}{\sqrt{\sum_{i=1}^{n}(A_i-\bar{A})^2}\sqrt{\sum_{i=1}^{n}(G_i-\bar{G})^2}} \quad (9)$$

where, $\bar{A}$ and $\bar{G}$ represent the mean values of the altimetry-derived and in situ water level series, respectively. This coefficient quantifies the degree to which the radar altimeter captures the variability of water level fluctuations observed in the gauge data. Values close to 1 indicate a strong correspondence in temporal dynamics.

In addition, the Nash–Sutcliffe efficiency coefficient (NSE) (Nash & Sutcliffe, 1970) was used to evaluate the agreement between altimetry-derived and in situ measurements (Eq. (10)):

$$NSE = 1 - \frac{\sum_{i=1}^{n}(A_i-G_i)^2}{\sum_{i=1}^{n}(G_i-\bar{G})^2} \quad (10)$$

NSE quantifies how well altimetry-derived values reproduce the variability observed in ground-based measurements. An NSE value of 1 indicates perfect agreement, a value of 0 suggests that the model performs no better than the mean of the observations, and negative values indicate unsatisfactory predictive performance.

3.5. NDWI extracted surface area uncertainty assessment

Because no independent reference datasets describing reservoir surface area were available for the study area, uncertainty associated with the extracted water-covered areas was estimated using a shoreline displacement approach. Considering the 3 m spatial resolution of PlanetScope imagery, ±3 m and ±6 m buffer scenarios were applied to the minimum and maximum reservoir extents observed during the study period.

For each case, surface area uncertainty (U_A) was calculated as half of the difference between the outward buffered ($A_{outward}$) and inward buffered (A_{inward}) polygon areas according to Eq. (11):

$$U_A = \frac{A_{outward}-A_{inward}}{2} \quad (11)$$

Relative uncertainty ($U_A(\%)$) was additionally calculated using Eq. (12):

$$U_A(\%) = \frac{U_A}{A} \times 100 \quad (12)$$

where A is the NDWI mapped reservoir area (km^2).

4. RESULTS

4.1. Validation of Sentinel-3A water levels

Altimeter–derived water level measurements were compared with hydrological station observations over the 93 months of the study period. The validation metrics indicate a small systematic offset and low discrepancies between the two datasets, with Bias = 0.097 m, RMSE = 0.192 m, Pearson's r = 0.997, and NSE = 0.993. In addition to the monthly comparison, the data were aggregated to an annual scale and evaluated using the same indicators. At this temporal resolution, Bias remained nearly unchanged (0.099 m), while RMSE decreased to 0.114 m, indicating that a portion of the differences observed in the monthly series is associated with short-term fluctuations rather than persistent deviations.

The scatter plot of monthly observations (**Fig. 3**) shows that, across the full range of water levels, most points cluster closely around the 1:1 reference line. Larger deviations are observed at lower water levels, likely due to mixed land–water returns recorded by the altimeter under low-stage conditions. The overall positive bias indicates that satellite-derived water levels are, on average, slightly higher than the corresponding station measurements. However, this deviation is small relative to the total water level range of nearly 10 m observed during the study period and does not significantly affect the characterization of seasonal dynamics.

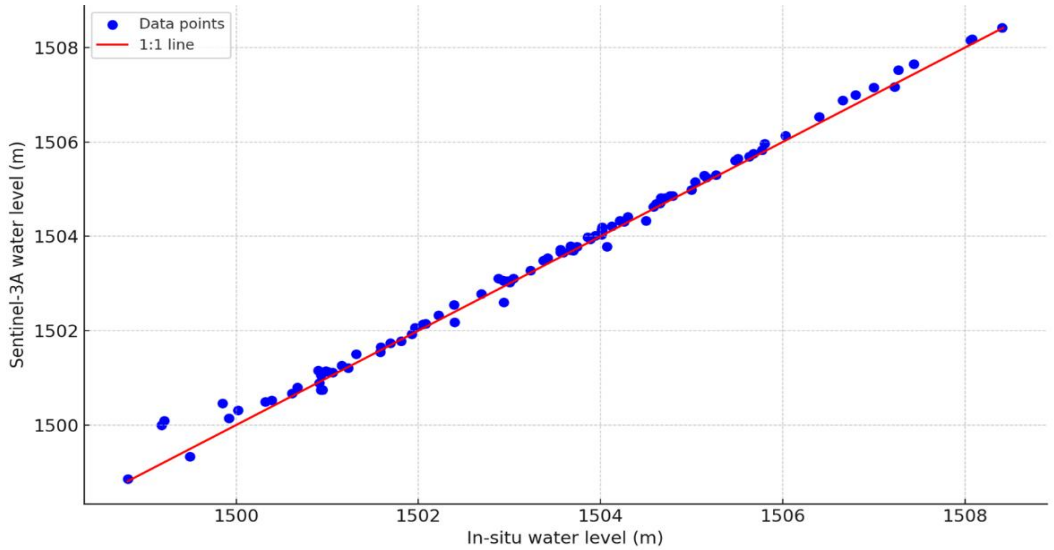

Fig. 3. Sentinel-3A altimetry vs in situ measurements monthly scatter plot.

Analysis of water level variations in the Tsalka Reservoir (**Fig. 4**), based on hydrological station and radar altimeter data, shows that both datasets follow the same sequence of water level increase and decrease. Differences between the curves are most evident during periods of rapid change, particularly during the reservoir filling phase in spring and the recession phase in autumn. The RMSE between Sentinel-3 and in situ water levels was used as an estimate of water level uncertainty. Therefore, the uncertainty of altimetry-derived water levels was considered to be approximately ±0.192 m.

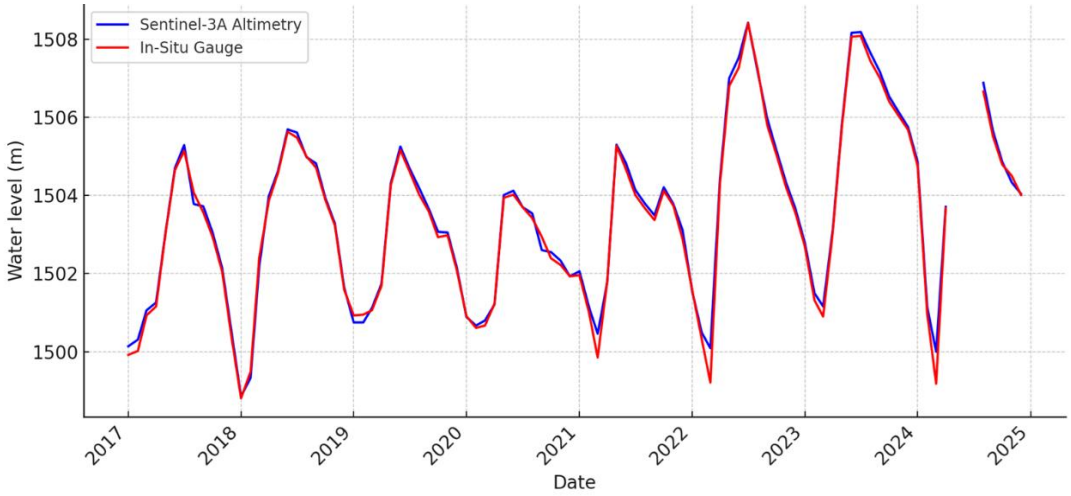

Fig. 4. Superposition of water levels from Sentinel-3A with in situ measurements.

4.2. Seasonal and interannual variability of reservoir water levels

The results indicate that the Tsalka Reservoir exhibits a pronounced seasonal cycle and significant interannual variability (**Fig. 5**). Throughout the study period, the lowest water levels were generally observed from mid-winter to early spring, typically between January and April. A rapid increase begins in mid-spring, with maximum levels reached between June and August. Following the peak, water levels gradually decline during autumn and early winter.

From 2017 to 2019, interannual fluctuations were relatively moderate, with summer maxima slightly exceeding 1505 m and winter minima generally ranging between 1499 and 1500 m. The overall minimum of the study period was recorded in 2018, reaching 1498.86 m. In 2020, a reduced amplitude was observed, with water levels remaining within approximately 1501–1504 m.

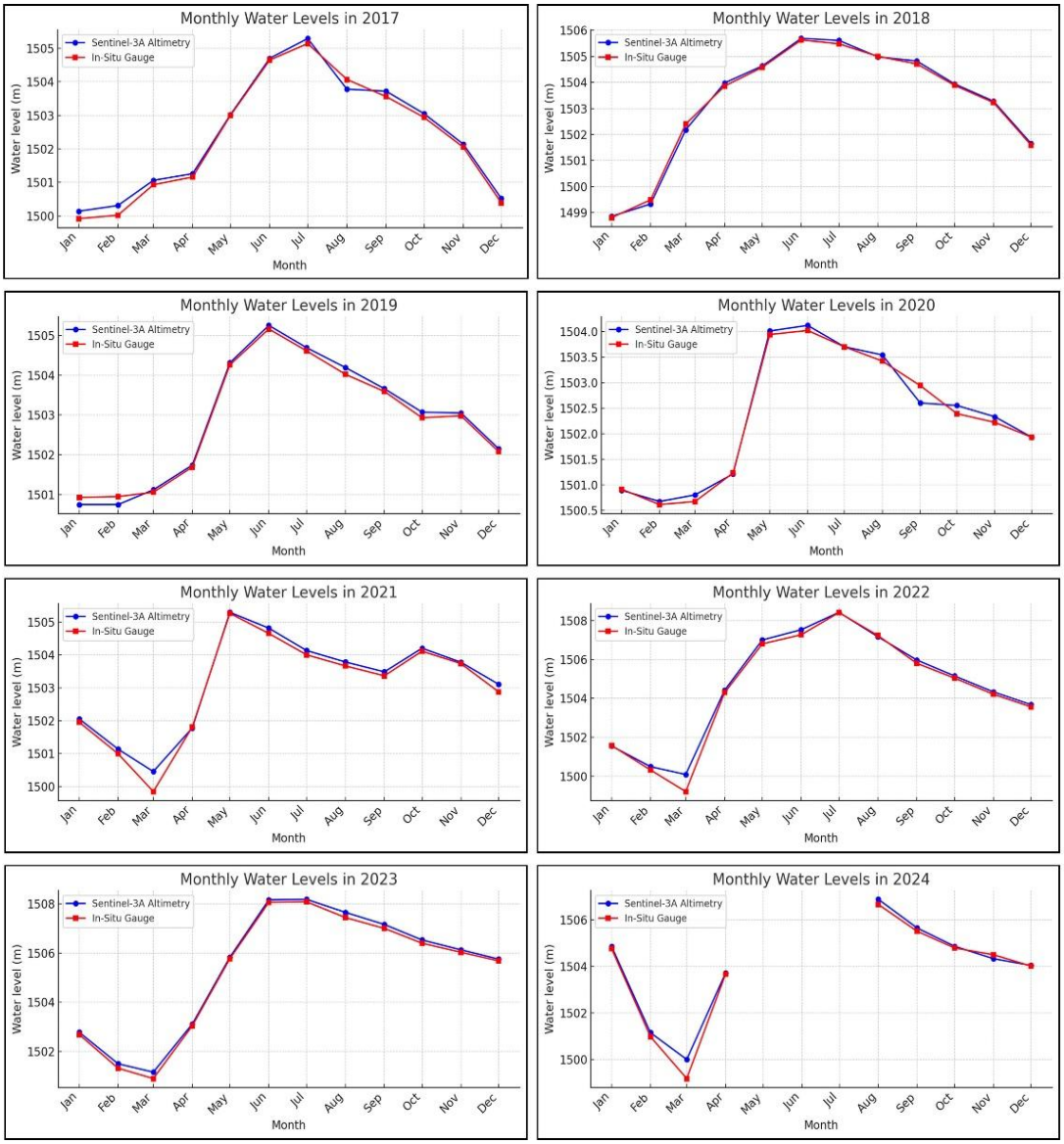

Fig. 5. Annual water level variations in Tsalka Reservoir from 2017 to 2024 – superposition of Sentinel-3A altimetry with in situ measurements.

Despite relatively weak seasonal variability, rapid filling events occurred in late spring in both 2020 and 2021. The largest fluctuations were recorded in 2022, when water levels declined to one of the lowest values of the study period and subsequently increased rapidly to the overall maximum (1508.42 m). Elevated water levels were also observed in 2023; however, in this case, the hydrograph indicates that these conditions were sustained over a longer period. As noted, altimetry data for 2024 are incomplete, with no observations available for May–July; nevertheless, the available monthly measurements and gauging station data indicate a seasonal pattern comparable to previous years.

The boxplot grouped by calendar month (**Fig. 6**) summarizes the annual cycle of the Tsalka Reservoir for the period 2017–2024.

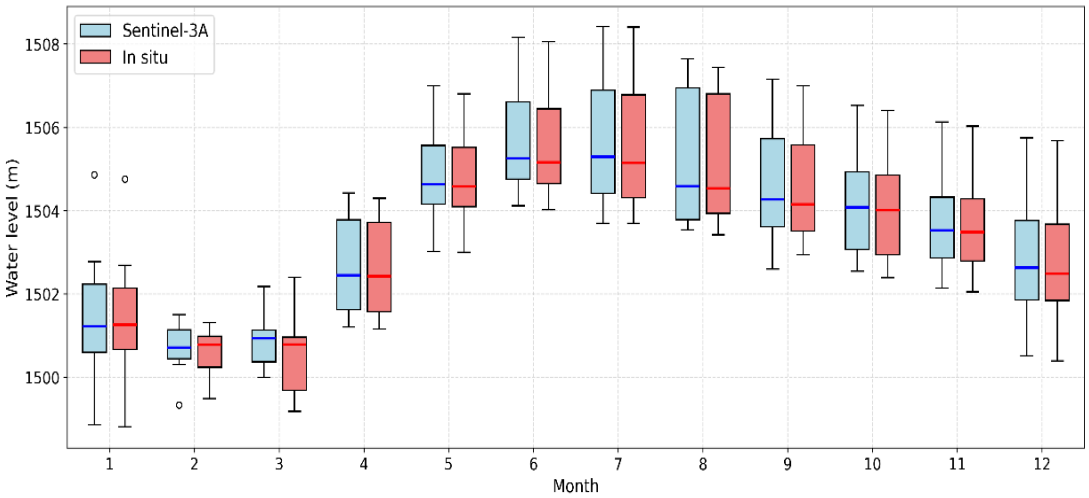

Fig. 6. Monthly water level variations from 2017 to 2024 – Sentinel-3A and in situ measurements.

February and March exhibit the lowest median values and include the minimum water levels in the dataset. From April onward, the distribution increases rapidly, reflecting the onset of reservoir filling. The highest median levels are observed in June and July. These months, together with August, display relatively high variability, as they encompass both moderate conditions and extreme high-water levels recorded in 2022 and 2023. From August to November, median values gradually decline, corresponding to the recession phase. The boxplot also highlights the asymmetry of the reservoir regime. The rise from minimum to maximum water levels occurs over a relatively short period (approximately three to four months), whereas the subsequent decline extends over a longer duration.

4.3. Variability of water-covered area and stage-area relationship

The wide range of water level fluctuations in the Tsalka Reservoir results in pronounced variations in water-covered area. **Fig. 7** illustrates the contrast between the minimum and maximum extents of inundation observed during the study period.

In January 2018, the area covered by water was 5.69 km², mainly confined to the deepest central part of the basin. By July 2022, at peak water levels, the area had increased to 24.54 km², representing more than a fourfold expansion. Spatial analysis of surface area variability indicates that even small changes in water level within certain ranges result in substantial horizontal shifts of the shoreline. The expansion of the reservoir area occurs primarily across the relatively shallow western and northern sectors. In contrast, the southern shoreline is characterized by rocky and steeper terrain, and therefore contributes minimally to the overall increase in surface area. At low water levels, the shoreline becomes fragmented, and the reservoir is divided into several disconnected sections. In the northern part, where water persists under these conditions, small lakes existed prior to reservoir construction. As the water level rises, these sectors reconnect and form a continuous water surface.

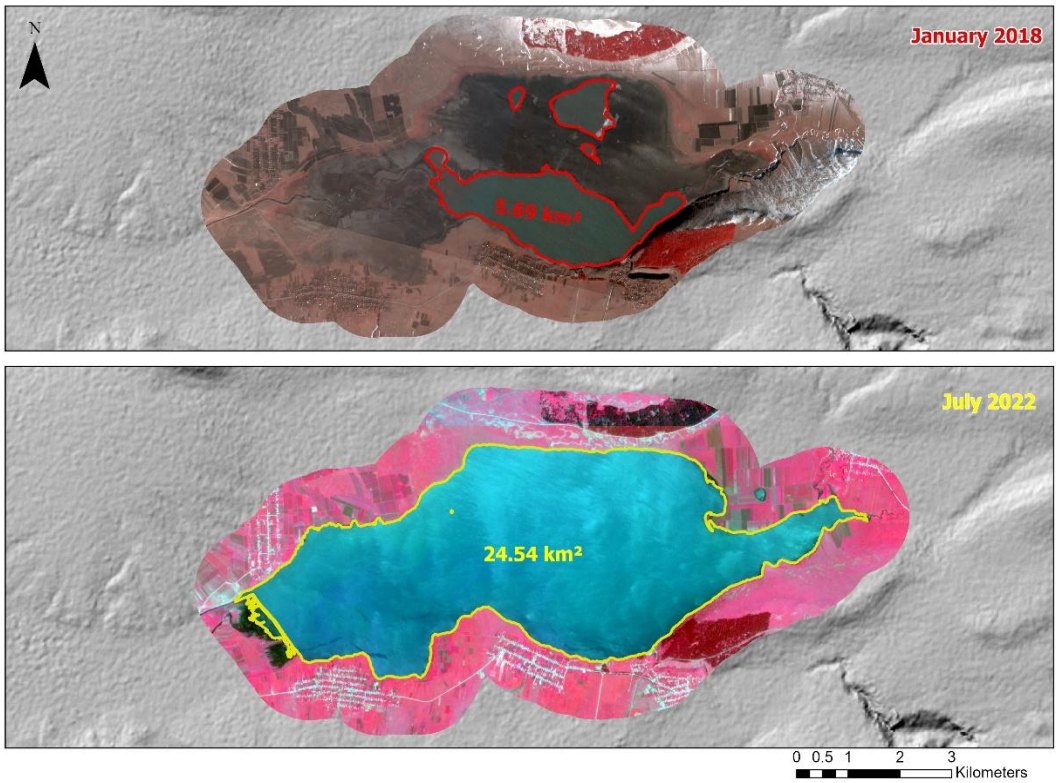

Fig. 7. Minimum and maximum reservoir extent observed during the study period (PlanetScope false color composites).

According to the Surface area uncertainty assessment results, under the ±3 m scenario, uncertainty was estimated as 0.06 km² for the minimum reservoir extent and 0.09 km² for the maximum extent, corresponding to 1.05% and 0.36% of the mapped area, respectively. Under the more conservative ±6 m scenario, uncertainty increased to 0.12 km² and 0.19 km², corresponding to 2.10% and 0.77%, respectively. The results indicate that relative uncertainty is considerably higher during low-water conditions, where shoreline fragmentation and narrow inundated zones increase sensitivity to shoreline displacement. Conversely, uncertainty decreases during high water stages due to the formation of a more continuous water surface and the reduced proportional influence of shoreline variability on the total mapped area.

The potential impact of temporal mismatch between Sentinel-3 and PlanetScope observations was additionally quantified using in situ water level measurements corresponding to paired acquisition dates. The analysis demonstrated that the mean temporal offset was 1.53 days (maximum 5 days), while the mean corresponding water level difference was 0.063 m, with a median difference of 0.02 m and standard deviation of 0.14 m. These results indicate that short-term water level variations between paired observations were generally minor, suggesting that the adopted ±5-day pairing window introduced limited uncertainty into the derived stage–area relationship.

The relationship between water level and surface area is nonlinear and exhibits a sigmoidal pattern (**Fig. 8**). Although the fitted 4PL model adequately reproduces the overall nonlinear stage–area relationship, the distribution of observations is uneven across the full range of reservoir stages, with most measurements concentrated within intermediate water levels. As described in the Methods section, the presented curve is derived solely from observations within the study period and does not represent the full range of possible reservoir storage conditions. Slight deviations observed during low and high-water conditions may additionally reflect increased shoreline uncertainty, fragmented inundation geometry, and limited observation density near extreme reservoir stages.

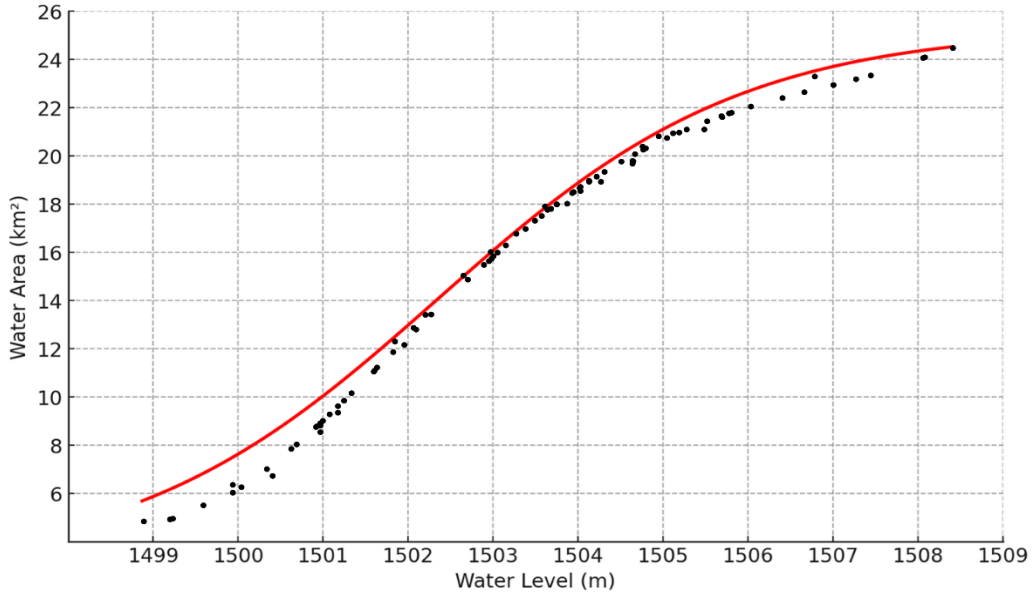

Fig. 8. Relationship between reservoir water level and water-covered area derived from Sentinel-3 altimetry and PlanetScope imagery during the 2017–2024 study period. Black points represent level–area pairs, while the red curve shows the fitted four-parameter logistic (4PL) stage–area relationship.

At low water levels, increases in stage result in relatively small changes in surface area, as the reservoir remains confined to the deeper central part of the basin. Within the intermediate range (approximately 1502–1505 m), the curve steepens, indicating rapid inundation of the shallow marginal zones. Above approximately 1506 m, the curve gradually flattens, indicating that further increases in water level continue to enlarge the reservoir extent, but at a reduced rate.

5. DISCUSSION

A comparison of Sentinel-3A SRAL water levels with in situ observations demonstrates that the radar altimeter captures the hydrodynamic behavior of the Tsalka Reservoir with high accuracy, even under complex topographic conditions of the study area. The obtained statistical metrics (RMSE = 0.192 m, Bias = 0.097 m, r = 0.997, NSE = 0.993) indicate that discrepancies between the two datasets are minor relative to the full range of observed water levels and do not influence the interpretation of seasonal and interannual dynamics. Similar performance of Sentinel-3 has been reported in recent studies, which show that, under favorable conditions, sub-decimeter to decimeter-level accuracy can be achieved for inland water bodies (Nielsen, Andersen, and Ranndal, 2020; Jiang et al., 2020; Xu et al., 2024).

The accuracy of the results depends strongly on the data processing methodology. As demonstrated by the obtained results, the methods applied in this study effectively reduced the influence of anomalous measurements on overall accuracy. In particular, the use of a dynamic virtual station, iterative outlier filtering, and median-based aggregation is well suited for reservoirs such as Tsalka, where seasonal shoreline migration increases the likelihood of mixed land–water returns. The sensitivity of radar altimetry to such conditions, including retracker performance and waveform heterogeneity, has been widely discussed in the context of applications related to inland water bodies (Taburet et al., 2020; Nielsen, Andersen, and Ranndal, 2020). For targets like the Tsalka Reservoir, where specular reflections from the water surface may be contaminated by signals from surrounding terrain, the use of the ICE-1 (OCOG-type) retracker remains an appropriate choice.

The water level dynamics identified in this study reflect a regulated reservoir system, characterized by a clear seasonal pattern and distinct interannual variability. Radar altimetry data effectively capture both gradual seasonal trends and more pronounced deviations. These findings indicate that, despite its 27-day repeat cycle, Sentinel-3 is capable of reliably representing the dynamics of a medium-sized reservoir, particularly when extended time series are considered.

The seasonal and interannual behavior of the reservoir generally corresponds to the climatic regime of the study area, where increased precipitation and rising air temperatures during spring and early summer likely contribute to enhanced inflow and reservoir filling. In contrast, declining water levels during late summer and autumn are consistent with reduced precipitation input. The minimum reservoir level and surface extent observed in January 2018 correspond to one of the lowest mean air temperatures recorded for the preceding October–December period (2.5 °C according to ERA5-Land 2 m temperature data), as well as one of the lowest cumulative precipitation totals for the same period (179.26 mm based on GPM data). Conversely, the maximum reservoir extent and water level observed in 2022 followed the highest cumulative March–June precipitation total during the study period (394.76 mm), while the mean air temperature for the same period reached 6.7 °C. However, the absence of reservoir operation records for the study period limits the ability to separate the effects of climatic forcing and operational regulation on the observed reservoir dynamics.

The integration of high spatial resolution PlanetScope optical imagery enabled detailed mapping of the reservoir shoreline dynamics. In addition, the short revisit interval of this satellite constellation reduced temporal discrepancies relative to the altimetry measurements. However, the limitations of optical data and applied methods for surface area extraction should also be acknowledged. Uncertainties in surface area estimates are primarily associated with threshold selection, mixed pixels along the shoreline, and seasonal snow and ice cover, which makes the spectral separation of water more challenging. The uncertainty assessment performed in this study indicates that the influence of shoreline displacement becomes proportionally more significant during low-water conditions, when fragmented shoreline increase the sensitivity of mapped surface area to positional inaccuracies. Conversely, uncertainty decreases during high-water stages due to the formation of a more continuous water surface.

From a broader perspective, the results of this study confirm the effectiveness of radar altimetry combined with high-resolution optical imagery, as well as the applied methodological framework, for monitoring inland water bodies in regions where in situ data are limited or unavailable. In the Georgian context, where systematic hydrological observations of lakes and reservoirs are largely absent, the approach presented in this study provides a viable alternative for estimating certain hydrometric parameters and reconstructing the dynamics of inland waters. However, reliance on a single satellite mission imposes constraints on both spatial and temporal coverage. In the future, the combined use of other altimetry missions, such as ICESat-2, CryoSat-2, Topex/Poseidon, ENVISAT, SWOT, Sentinel-6, etc., will enable monitoring of a larger number of water bodies, especially when it comes to small and morphologically complex systems (Kwanghee et al., 2024).

Despite the overall effectiveness of the proposed approach, several limitations should be acknowledged. As noted in previous sections, only a single Sentinel-3A ground track intersects the Tsalka Reservoir, which limits the spatial representativeness of the data and increases the sensitivity of altimetry measurements to local conditions along the track, potentially introducing errors. Nevertheless, previous studies have demonstrated that reliable water level retrievals can still be achieved using a single Sentinel-3A ground track. For example, Frappart et al. (2021) reported R^2 values exceeding 0.9 and RMSE values below 0.1 m for Lake Thun in Switzerland. The 27-day repeat cycle constrains the ability to capture short-term fluctuations associated with rapid reservoir filling (e.g., following intense precipitation events within the catchment) and drawdown (e.g., due to operational releases for hydropower generation). In addition, seasonal ice cover in certain years, as well as incomplete data for 2024, may introduce additional uncertainties in the analysis. These limitations emphasize the importance of multi-mission integration and, where possible, the incorporation of auxiliary data sources (e.g., meteorological observations and reservoir operation records).

6. CONCLUSIONS

In this study, surface area and level variations of the Tsalka (Khrami) Reservoir were assessed for the period 2017–2024 using Sentinel-3 radar altimetry and PlanetScope optical imagery. The accuracy of the altimetry-derived time series, obtained from the Level-2 GDR product, was validated against in situ hydrological station data. The resulting statistical metrics indicate a high level of agreement between satellite-based and ground observations, confirming the reliability of the data and methodology used in the study for monitoring medium-sized reservoirs, particularly in regions where in situ data are sparse or not regularly available.

Time series analysis of water levels shows a clear seasonal regime in the Tsalka Reservoir, characterized by rising water levels during the spring and summer period with peak levels typically reached in late summer. This phase is followed by a gradual decline throughout autumn and winter. During the study period, the maximum annual amplitude of water levels reached approximately 10 m, indicating the highly dynamic nature of the reservoir system.

The integration of high spatial and temporal resolution optical imagery enabled not only the assessment of water levels but also the analysis of associated shoreline dynamics. Although the design surface area of the Tsalka Reservoir exceeds 33 km², this limit was not reached during the 8-year study period, with a maximum observed area of 24.54 km². Despite this, the Tsalka Reservoir remains the largest artificial reservoir in the country even based on observed maximum water-covered extent. Notably, the difference between the maximum (2022) and minimum (2018) recorded areas is 18.85 km², indicating strong variability in reservoir extent.

Overall, the results demonstrate that Sentinel-3 altimetry provides sufficient accuracy for monitoring medium-sized inland water bodies, while high spatial and temporal resolution PlanetScope imagery is well suited for deriving surface area in support of altimetry observations. In the context of expanding spatial coverage and ongoing technological advances in current and forthcoming satellite altimetry missions, the approach presented in this study constitutes a cost-effective framework that can be effectively integrated into the development of a national inland water monitoring system in Georgia.

ACKNOWLEDGMENTS

The Authors are grateful to the JSC “KHRAMHESI I” for providing Tsalka Reservoir in situ water level observations.

REFERENCES

Alcaras, E., Amoroso, P.P., Figliomeni, F.G., Parente, C. and Prezioso, G. (2022) Accuracy evaluation of coastline extraction methods in remote sensing: a smart procedure for Sentinel-2 images, *The International Archives of the Photogrammetry, Remote Sensing and Spatial Information Sciences*, XLVIII-4/W3-2022, pp. 13–19. Available from: https://doi.org/10.5194/isprs-archives-XLVIII-4-W3-2022-13-2022

An, Z., Chen, P., Tang, F., Yang, X., Wang, R. and Wang, Z. (2022) Evaluating the performance of seven ongoing satellite altimetry missions for measuring inland water levels of the Great Lakes, *Sensors*, 22, 9718. Available from: https://doi.org/10.3390/s22249718

Bazzi, H., Baghdadi, N., Ngo, Y.-N., Normandin, C., Frappart, F. and Cazals, C. (2025) Assessing SWOT interferometric SAR altimetry for inland water monitoring: insights from Lake Léman, *Frontiers in Remote Sensing*, 6, 1572114. Available from: https://doi.org/10.3389/frsen.2025.1572114

Chen, J. and Duan, Z. (2022) Monitoring spatial-temporal variations of lake level in Western China using ICESat-1 and CryoSat-2 satellite altimetry, *Remote Sensing*, 14, 5709. Available from: https://doi.org/10.3390/rs14225709

Cheng, C., Zhang, F., Li, X., Tan, M.L., Kumar, P., Johnson, B.A., Shi, J., Zhao, Q. and Liu, C. (2023) Variations in water storage of Bosten Lake, China, over the last two decades based on multi-source satellite data, *Journal of Hydrology: Regional Studies*, 49, 101496. Available from: https://doi.org/10.1016/j.ejrh.2023.101496

Crétaux, J.-F., Nielsen, K., Frappart, F., Papa, F., Calmant, S. and Benveniste, J. (2017) Hydrological applications of satellite altimetry: rivers, lakes, man-made reservoirs, inundated areas, in Stammer, D. and Cazenave, A. (eds.) *Satellite altimetry over oceans and land surfaces*. Boca Raton, FL: CRC Press

Dalla Torre, D., Di Marco, N., Menapace, A., Avesani, D., Righetti, M. and Majone, B. (2024) Suitability of ERA5-Land reanalysis dataset for hydrological modelling in the Alpine region, *Journal of Hydrology: Regional Studies*, 52, 101718. Available from: https://doi.org/10.1016/j.ejrh.2024.101718

El Orfi, T., El Gachi, M., Lebaut, S. and Haidu, I. (2025) Monitoring the water surface dynamics of four Mediterranean mountain lakes in the Middle Atlas (Morocco) using Landsat imagery in a global change context, *Journal of Hydrology: Regional Studies*, 60, 102516. Available from: https://doi.org/10.1016/j.ejrh.2025.102516

Fernandes, M.J., Lázaro, C., Nunes, A.L. and Scharroo, R. (2014) Atmospheric corrections for altimetry studies over inland water, *Remote Sensing*, 6, pp. 4952–4997. Available from: https://doi.org/10.3390/rs6064952

Frappart, F., Blumstein, D., Cazenave, A., Ramillien, G., Birol, F., Morrow, R. and Rémy, F. (2017) Satellite altimetry: principles and applications in Earth sciences, in *Wiley Encyclopedia of Electrical and Electronics Engineering*. Hoboken, NJ: John Wiley & Sons, Inc., pp. 1–25. ISBN 047134608X

Frappart, F., Blarel, F., Fayad, I., Bergé-Nguyen, M., Crétaux, J.-F., Shu, S., Schregenberger, J. and Baghdadi, N. (2021) Evaluation of the performances of radar and lidar altimetry missions for water level retrievals in mountainous environment: the case of the Swiss lakes, *Remote Sensing*, 13(11), 2196. Available from: https://doi.org/10.3390/rs13112196

Haidu, I., El Orfi, T., Magyari-Sáska, Z., Lebaut, S. and El Gachi, M. (2024) Modeling the long-term variability in the surfaces of three lakes in Morocco with limited remote sensing image sources, *Remote Sensing*, 16(17), 3133. Available from: https://doi.org/10.3390/rs16173133

Han, K., Kim, S., Mehrotra, R. and Sharma, A. (2024) Enhanced water level monitoring for small and complex inland water bodies using multi-satellite remote sensing, *Environmental Modelling & Software*, 180, 106169. Available from: https://doi.org/10.1016/j.envsoft.2024.106169

Iordanishvili, K., Iordanishvili, I., Iremashvili, I. and Kandelaki, N. (2023) *Peculiarities of engineering-ecological problems of mountain and foothill reservoirs* (in Georgian). Tbilisi: Sachino Publishing House.

Jamali, S., Zaidi, A. and Ali, T. (2025) Integrating satellite altimetry and SAR technology for Manchar Lake water monitoring, *Discover Water*, 5, 114. Available from: https://doi.org/10.1007/s43832-025-00292-0

Jawad, M., Bhattacharya, B., Young, A. and van Andel, S.J. (2024) Evaluation of near real-time Global Precipitation Measurement (GPM) precipitation products for hydrological modelling and flood inundation mapping of sparsely gauged large transboundary basins—A case study of the Brahmaputra Basin, *Remote Sensing*, 16(10), 1756. Available from: https://doi.org/10.3390/rs16101756

Jiang, L., Nielsen, K., Dinardo, S., Andersen, O.B. and Bauer-Gottwein, P. (2020) Evaluation of Sentinel-3 SRAL SAR altimetry over Chinese rivers, *Remote Sensing of Environment*, 237, 111546. Available from: https://doi.org/10.1016/j.rse.2019.111546

Kossieris, S., Tsiakos, V., Tsimiklis, G. and Amditis, A. (2024) Inland water level monitoring from satellite observations: a scoping review of current advances and future opportunities, *Remote Sensing*, 16, 1181. Available from: https://doi.org/10.3390/rs16071181

Luo, S., Song, C., Ke, L., Zhan, P., Fan, C. and Liu, K. *et al.* (2022) Satellite laser altimetry reveals a net water mass gain in global lakes with spatial heterogeneity in the early 21st century, *Geophysical Research Letters*, 49, e2021GL096676. Available from: https://doi.org/10.1029/2021GL096676

McFeeters, S.K. (1996) The use of the normalized difference water index (NDWI) in the delineation of open water features, *International Journal of Remote Sensing*, 17(7), pp. 1425–1432. Available from: https://doi.org/10.1080/01431169608948714

Nash, J.E. and Sutcliffe, J.V. (1970) River flow forecasting through conceptual models part I — A discussion of principles, *Journal of Hydrology*, 10(3), pp. 282–290. Available from: https://doi.org/10.1016/0022-1694(70)90255-6

Nielsen, K., Andersen, O.B. and Ranndal, H. (2020) Validation of Sentinel-3A based lake level over US and Canada, *Remote Sensing*, 12, 2835. Available from: https://doi.org/10.3390/rs12172835

Taburet, N., Zawadzki, L., Vayre, M., Blumstein, D., Le Gac, S., Boy, F. *et al.* (2020) S3MPC: improvement on inland water tracking and water level monitoring from the OLTC onboard Sentinel-3 altimeters, *Remote Sensing*, 12, 3055. Available from: https://doi.org/10.3390/rs12183055

Tang, F., Chen, P., An, Z., Xiong, M., Chen, H. and Qiu, L. (2023) A dual-threshold algorithm for ice-covered lake water level retrieval using Sentinel-3 SAR altimetry waveforms, *Sensors*, 23, 9724. Available from: https://doi.org/10.3390/s23249724

Tielidze, L.G., Nadaraia, A., Kumladze, R.M., Cook, S.J., Lobjanidze, M., Liu, Q., Megrelidze, I., Mackintosh, A.N. and Imnadze, G. (2025) Post-Little Ice Age shrinkage of the Tsaneri–Nageba glacier system and recent proglacial lake evolution in the Georgian Caucasus, *Water*, 17(22), 3209. Available from: https://doi.org/10.3390/w17223209

Tielidze, L.G., Mackintosh, A.N., Gavashelishvili, A., Gadrani, L., Nadaraia, A. and Elashvili, M. (2025) Post-Little Ice Age equilibrium-line altitude and temperature changes in the Greater Caucasus based on small glaciers, *Remote Sensing*, 17(9), 1486. Available from: https://doi.org/10.3390/rs17091486

Van, L.N., Nguyen, G.V., Kim, Y., Do, M.T.T., Kwon, S., Lee, J. and Lee, G. (2025) Rapid urban flood detection using PlanetScope imagery and thresholding methods, *Water*, 17, 1005. Available from: https://doi.org/10.3390/w17071005

Wang, J. and Gao, Y. (2025) Monitoring long-term water storage of lakes and reservoirs in arid ungauged basin based on underwater topography derived from multi-source satellite data, *Science of the Total Environment*, 966, 178662. Available from: https://doi.org/10.1016/j.scitotenv.2025.178662

Wang, X., Guo, X., Yang, C., Liu, Q., Wei, J., Zhang, Y. *et al.* (2020) Glacial Lake inventory of high-mountain Asia in 1990 and 2018 derived from Landsat images, *Earth System Science Data*, 12, pp. 2169–2182. Available from: https://doi.org/10.5194/essd-12-2169-2020

Woolway, R.I., Kraemer, B.M., Lenters, J.D., Merchant, C.J., O'Reilly, C.M. and Sharma, S. (2020) Global Lake responses to climate change, *Nature Reviews Earth & Environment*, 1, pp. 388–403. Available from: https://doi.org/10.1038/s43017-020-0067-5

Xu, J., Xia, M., Ferreira, V.G., Wang, D. and Liu, C. (2024) Estimating and assessing monthly water level changes of reservoirs and lakes in Jiangsu Province using Sentinel-3 radar altimetry data, *Remote Sensing*, 16, 808. Available from: https://doi.org/10.3390/rs16050808

Zeng, F., Song, C., Cao, Z., Xue, K., Lu, S., Chen, T. and Liu, K. (2023) Monitoring inland water via Sentinel satellite constellation: a review and perspective, *ISPRS Journal of Photogrammetry and Remote Sensing*, 204, pp. 340–361. Available from: https://doi.org/10.1016/j.isprsjprs.2023.09.011